JOURNAL OF AIRCRAFT
Vol. 30, No. 6, Nov.–Dec. 1993

Aerodynamic Performance Effects due to Small Leading-Edge Ice (Roughness) on Wings and Tails

Walter O. Valarezo* and Frank T. Lynch†
McDonnell Douglas Corporation, Long Beach, California 90846
and
Robert J. McGhee‡
NASA Langley Research Center, Hampton, Virginia 23681

Systematic experimental studies have been carried out to establish the aerodynamic impact of very small leading-edge simulated ice (roughness) formations on lifting surfaces. The geometries studied include single-element configurations (airfoil and three-dimensional tail) as well as multielement high-lift airfoil geometries. Emphasis in these studies was placed on obtaining results at high Reynolds numbers to insure the applicability of the findings to full-scale situations. It has been found that the well-known Brumby correlation for the adverse lift impact of discrete roughness elements at the leading edge is not appropriate for cases representative of initial frost formation (i.e., distributed roughness). It has further been found that allowing initial ice formations, of a size required for removal by presently proposed de-icing systems, could lead to maximum lift losses of approximately 40% for single-element airfoils. Losses in angle-of-attack margin-to-stall are equally substantial—as high as 6 deg. Percentage losses for multielement airfoils are not as severe as for single-element configurations, but degradations of the angle of attack-to-stall margin are the same for both.

Nomenclature

C_p	=	pressure coefficient
k/c	=	ratio of roughness height to airfoil chord
M_0	=	freestream Mach number
R_N	=	Reynolds number based on chord
x/c	=	nondimensional coordinate
$\sqrt{x/c}$	=	stretched nondimensional coordinate
$\%\Delta C_{l\max}$	=	percent loss in maximum lift coefficient
α	=	angle of attack

I. Introduction

WE have learned from observations in icing tunnels that the initial ice accumulation on the leading edge of airfoils, particularly at temperatures just below freezing, looks very much like distributed roughness, with a disturbance height nominally equal to the thickness of the ice buildup. For some years, an empirical correlation originally assembled by Brumby[1] has been used to estimate the reductions in (1 g) maximum lift capability caused by this leading-edge roughness, and therefore, to set limits for the amount of leading-edge ice buildup (or residual) that might be permitted if de-icing systems are to be used as alternatives to the widely used anti-icing systems with their demanding engine bleed-air requirements. Use of this correlation (Fig. 1) implied that if the thickness (k/c) of the ice buildup or residual was kept below 6×10^{-5} for installations without auxiliary leading-edge devices, or below 4×10^{-4} when leading-edge devices are deployed, then the reductions in (1 g) maximum lift would be less than 5% (about 2% in stall speed). While these "allowable" ice buildups were quite small, they were still in the range that was thought to be achievable by the developers of de-icing systems, particularly for large transport aircraft.

Received Oct. 17, 1991; revision received Aug. 10, 1992; accepted for publication Aug. 14, 1992.

*Principal Specialist, High Lift Aerodynamics. Senior Member AIAA.
†Manager, Aerodynamics Technology. Associate Fellow AIAA.
‡Head, Low-Turbulence Pressure Tunnel Section.

However, test results obtained in 1985[2] on a single-element airfoil over a wide Reynolds number range in the NASA Langley Low Turbulence Pressure Tunnel (LTPT)[3] provided an initial indication that usage of the Brumby correlation for the effects of leading-edge roughness significantly underestimated the loss in maximum lift that is experienced with a representative leading-edge ice buildup/residual (distributed roughness). As can be seen from Fig. 2, the 1985 test results for a k/c of 4×10^{-4} showed that the actual performance impact is closer to that expected when the entire upper surface is roughened. In fact, the loss in maximum lift (nearly 30%) was about three-quarters of that experienced with a simulated glaze ice buildup with horns. A computational study was conducted to estimate the effects of these small ice (roughness) buildups on the maximum lift capabilities of single-element

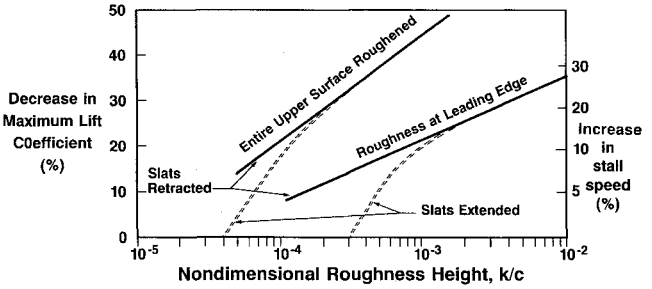

Fig. 1 Brumby correlation for roughness effects.

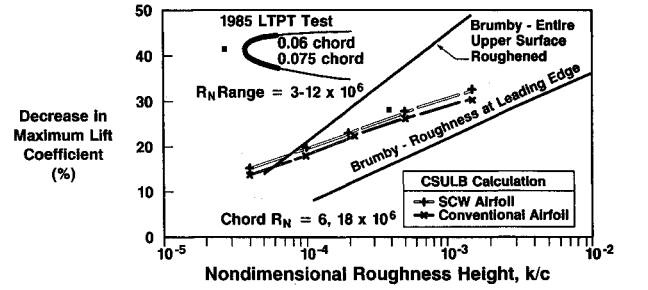

Fig. 2 Initial challenges to interpretation of Brumby roughness correlation for single-element airfoils.

airfoils for a range of roughness heights. These calculations, using an interactive boundary-layer method in which the turbulence model was modified as prescribed by Cebeci and Chang[4] to account for roughness effects, predicted losses in maximum lift capability that were close to those measured in the LTPT at the same roughness height. More importantly, the predicted results, also shown in Fig. 2, suggested that the maximum lift penalties at very small roughness heights ($k/c \sim 4 \times 10^{-5}$) were very substantial (~15%), not unlike those previously expected for having the entire upper surface roughened. As a consequence of these two new inputs, which clearly suggested that the adverse effects of very small ice (roughness) buildups on the leading edge of a single-element wing or tail could be significantly greater than previously estimated, McDonnell Douglas and NASA Langley Research Center expanded an ongoing cooperative test program in the LTPT to identify representative penalties over a range of small roughness heights for both single- and multielement airfoil configurations. Additional tests with very small roughness heights on a three-dimensional tail configuration were also carried out by McDonnell Douglas in the ONERA F-1 facility to help assess the two-dimensional LTPT results. The objective of this article is to demonstrate, by interpreting the subject test results, that there is no such thing as just a little bit of ice buildup on a wing or tail, in particular, with respect to de-icing applications. Analyses of the test data are presented which illustrate significant degradations in stall speeds and angle-of-attack margins for even the smallest amount of leading-edge ice buildup.

II. LTPT Test Facility

Nearly all the experimental results presented in this article were obtained from tests conducted in the LTPT. The LTPT is a single-return, closed-throat wind tunnel that can be operated at tunnel total pressures from near-vacuum to 10 atm.[3] A sketch of the tunnel circuit arrangement is shown in Fig. 3. The tunnel test section is 3-ft wide, 7.5-ft high, and 7.5-ft long, which, when combined with a 17.6-to-1 contraction ratio, makes the LTPT ideally suited for two-dimensional airfoil testing. The tunnel can obtain a maximum Reynolds number of 15×10^6 per foot at a Mach number of 0.24, although most of the testing reported here was conducted at a Mach number of 0.20 with Reynolds numbers of 10×10^6 per foot or less as indicated.

To ensure spanwise uniformity of the flowfield when testing high-lift airfoils at and below maximum lift coefficients, some form of tunnel sidewall boundary-layer control (BLC) is needed. The large adverse pressure gradients induced on the tunnel sidewalls by multielement high-lift airfoils, particularly near maximum lift, can cause the sidewall boundary layer to separate with a corresponding loss of spanwise uniformity of the flow on the airfoil surfaces, and can even lead to tunnel operating difficulties (surging, etc.). To provide adequate sidewall boundary-layer control for high-performance high-lift designs, a passive suction/venting system was developed and installed in the LTPT for this ongoing cooperative test program. This system consists of eight porous regions on each

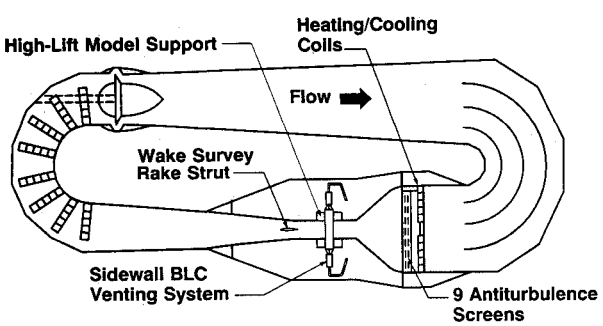

Fig. 3 Sketch of the Langley LTPT.

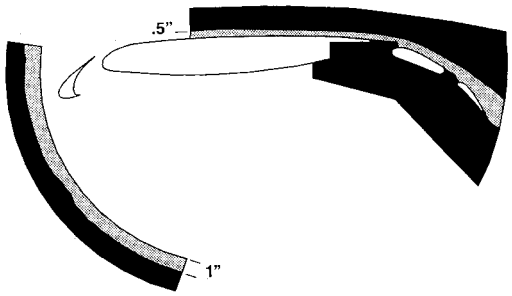

Fig. 4 Sidewall suction/venting area.

endplate through which the sidewall boundary layer is removed. The total porous area provided is illustrated in Fig. 4. The suction/venting process is driven by the higher-than-atmosphere test section total pressure, and the appropriate sidewall venting area for each type of configuration was developed by simply taping off portions of the porous endplate surfaces on both sidewalls. Selection of the proper pattern was based on an examination of spanwise pressure variations at several chordwise locations.

III. Model Geometries

The two-dimensional high-lift model used for this investigation of leading-edge distributed roughness effects in the LTPT was an aft-loaded-type airfoil equipped with a leading-edge slat and a two-segment flap. The cruise airfoil chord was 22 in., and the maximum thickness-chord ratio was 11.55%. Leading-edge slat, forward-flap segment, and aft-flap elements have respective chords of 14.48, 20.93, and 14.03% of the (unextended) cruise chord. The high-lift configuration with slat and two-segment flap deflected was instrumented with 142 centerline chordwise surface pressure taps which are used to determine the individual component and total configuration lift and pitching moment characteristics. Five spanwise rows of 10 taps each were also provided to monitor flow two-dimensionality. Leading-edge roughness effects at high-lift conditions were measured for a representative approach/landing configuration, with slat and flap deflections of 30, 35, and 15 deg, respectively. Optimized slat- and main-element-flap riggings (gaps and overhangs) were used for this portion of the study.

The three-dimensional horizontal tail model that was tested in the ONERA F-1 facility and used to validate the two-dimensional single-element airfoil roughness effects obtained in the LTPT, did not have aft-loaded airfoils. This configuration, which was mounted on top of a swept vertical tail, had an average maximum thickness-chord ratio of 11.37%, quarter-chord sweep angle of 33 deg, aspect ratio of 5, and taper ratio equal to 0.33.

IV. Single-Element Airfoil/Tail Test Results

To establish a sound basis for the experimental portion of this investigation, a water impingement analysis was performed for the single-element airfoil configuration to be tested in the LTPT to determine where to place the roughness elements to realistically simulate the effects of an initial ice build up. The method employed, the Douglas Viscous Neumann (DACVINE) panel method,[5] is capable of predicting the impingement of water droplets onto any desired surface by means of a particle trajectory and impingement calculation. The calculation takes into account the flowfield (multiple bodies), gravity, and the drag force on each particle, and is deemed appropriate to simulate the initial stages of ice accretion for the purpose of producing a realistic impingement pattern. Based on this study, for a range of conditions, it was determined that the pattern used in the 1985 LTPT test,[2] which covered the entire leading edge from 6% chord on the upper surface to 7.5% chord on the lower surface, was representative. Therefore, the same pattern was selected for the cur-

rent investigation to provide a basis for comparison. Incidentally, a posttest analysis using the modified LEWICE method[6] confirmed the validity of this choice.

Several roughness heights were applied to the leading edge of the aft-loaded single-element airfoil in the LTPT to simulate either the initial ice buildup which would occur in an icing encounter, or the residual which might remain after a de-icing system cycle. The roughness sizes (heights) used were 0.0016, 0.0045, and 0.0117 in., and resulted in nondimensional roughness heights (k/c) of 0.00007, 0.0002, and 0.00053, respectively. Carborundum grit was used for the largest, while Ballotini beads were utilized for the smaller two. Tests were conducted for an angle-of-attack range through stall for each roughness height, as well as the clean airfoil, at 0.20 Mach number for chord Reynolds numbers from 2.5 $\times$ 10^6 to 18 $\times$ 10^6. The resultant percentage loss in maximum lift capability for this Reynolds number variation is presented in Fig. 5. It can be seen that even the smallest roughness height tested caused a 20% loss in maximum lift capability for chord Reynolds numbers of 5 $\times$ 10^6 and above. The results obtained at a chord Reynolds number of 2.5 $\times$ 10^6 are clearly not representative, especially for the smallest roughness height. The reason for this nonrepresentative behavior at 2.5 $\times$ 10^6 Reynolds number is addressed subsequently in this section.

The measured reduction in maximum lift capability at chord Reynolds numbers of 5 $\times$ 10^6 and above is compared in Fig. 6 to the Brumby correlation[1] and the 1985 LTPT test results.[3] It can be seen that the present results are consistent with the previous LTPT measurements, and validate the trend predicted computationally, indicating the Brumby correlation for the entire upper surface roughened is clearly more representative of the effect of the typical initial leading-edge ice (roughness) buildup than the correlation based on more discrete leading-edge roughness elements, particularly for the smaller roughness heights. This behavior can probably be attributed to the failure of the boundary layer to negotiate the very large adverse pressure gradient that exists just aft of the leading edge that leads to flow breakdown and consequent earlier stall. The reduction in sustainable leading-edge peak pressure with increasing roughness height that was observed at 9 $\times$ 10^6 Reynolds number is illustrated in Fig. 7. Whereas, a peak suction pressure coefficient of -13 can be sustained prior to stall on the clean airfoil, -8 is the best that can be

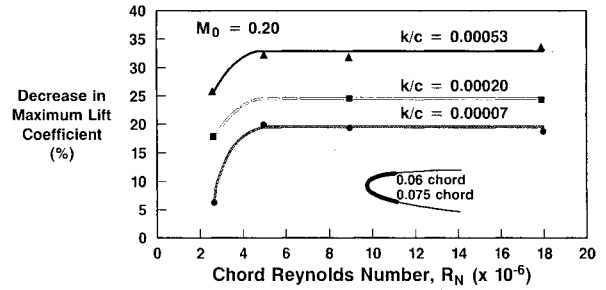

Fig. 5 Reynolds number effect on maximum lift loss due to leading-edge roughness on single-element airfoil.

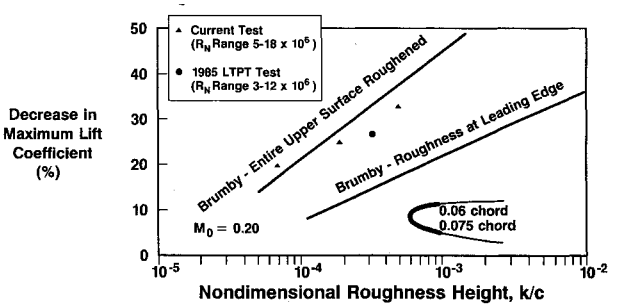

Fig. 6 Leading-edge roughness effects on single element airfoils in LTPT.

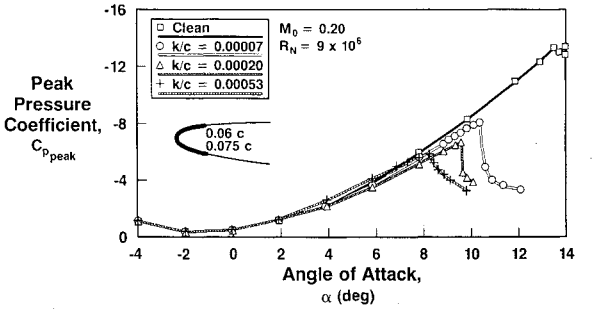

Fig. 7 Effect of leading-edge roughness on peak suction pressure for single-element airfoil.

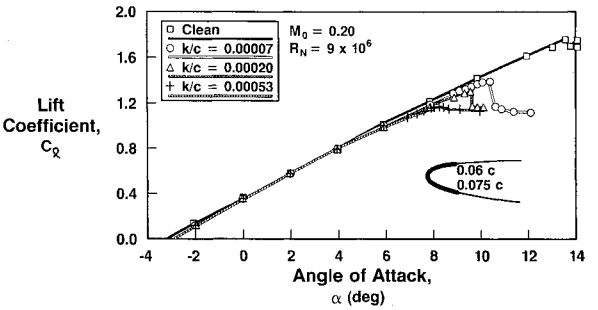

Fig. 8 Effect of leading-edge roughness on single-element airfoil lift characteristics.

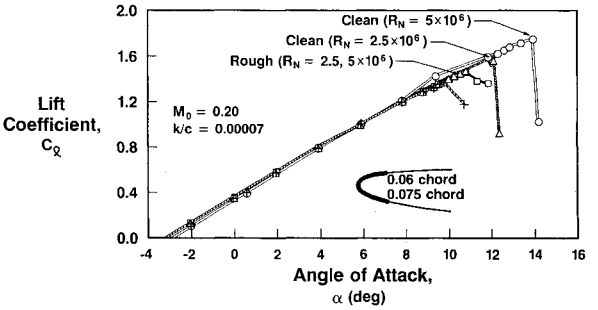

Fig. 9 Reynolds number effects on single-element airfoil lift characteristics with and without leading-edge roughness.

achieved with even the smallest roughness height. As can be seen from Fig. 7, and also as illustrated with the analogous lift curves shown in Fig. 8, the corresponding reduction in angle-of-attack margin to stall with the smallest roughness is over 3 deg, and increases to about 5 deg for the largest size tested.

As indicated earlier, too-low test Reynolds numbers can lead to erroneous indications of the reductions in maximum lift capability incurred with leading-edge ice (roughness) buildups. Results obtained in the present test program at a chord Reynolds number of 2.5 $\times$ 10^6 provide an example of how this occurs. The erroneous trend arises since the maximum lift without roughness is a strong function of Reynolds number, whereas the maximum lift with roughness is not. This is illustrated in Fig. 9 by the comparison of the lift curves for the clean airfoil, and with the smallest roughness applied, at chord Reynolds numbers of 2.5 $\times$ 10^6 and 5 $\times$ 10^6. The maximum lift with roughness applied are nearly identical for the two test Reynolds numbers, but the maximum lift at 2.5 $\times$ 10^6 Reynolds number on the clean airfoil is substantially lower due to the existence of a leading-edge laminar separation bubble that is not present at the higher Reynolds number. The existence of the laminar bubble at the lower Reynolds number is indicated by the bulge in the chordwise pressure distribution seen just aft of the suction peak in Fig. 10. Several attempts were made to eliminate this laminar bubble by fixing transition ahead of the bubble location, a technique reported

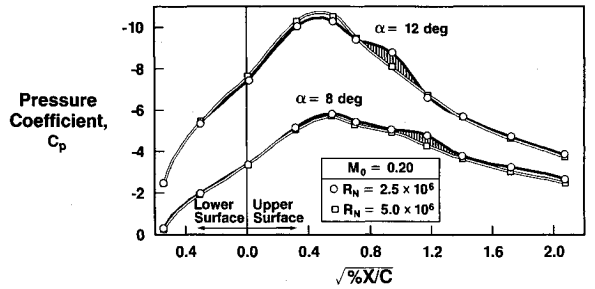

Fig. 10 Indicated laminar separation bubble on clean single-element airfoil at chord Reynolds number of 2.5 × 10⁶.

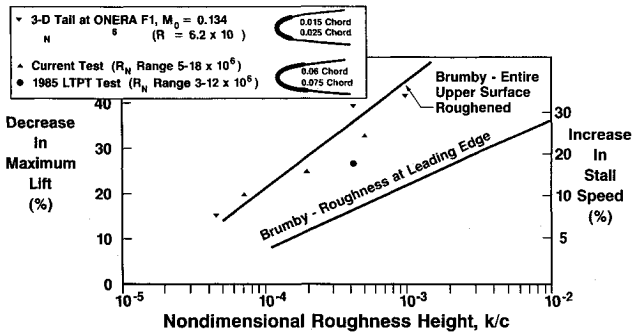

Fig. 11 Comparison of two- and three-dimensional test results for effect of roughness on maximum lift characteristics of single-element configurations.

to have been successfully used by other investigators in avoiding the nonrepresentative adverse consequences of having a bubble present. However, none of the present attempts were successful in increasing the clean airfoil maximum lift capability at this Reynolds number. Hence, extreme caution must be exercised when planning or interpreting results for any low-Reynolds number tests for leading-edge ice (roughness) buildup effects.

With any two-dimensional tunnel tests involving leading-edge flow separation characteristics, regardless of the test Reynolds number, there is always some concern regarding the direct applicability of the results to the real three-dimensional flow situations that exist on practical airplanes. To address this concern, several roughness heights were applied to the leading-edge region of a three-dimensional, single-element horizontal tail configuration that was being evaluated in the ONERA F-1 facility. The roughness sizes used resulted in nondimensional roughness heights (k/c) of 0.00004, 0.00036, and 0.00105, based on the tail mean aerodynamic chord (MAC). The roughness heights covered the leading edge from 1.5% chord on the suction surface to 2.5% chord on the pressure surface, a smaller coverage than used in the LTPT investigation. Test conditions were 0.134 Mach number, and a MAC Reynolds number of 6.2 × 10⁶. The corresponding percentage losses in maximum lift capability observed in these tests are compared to the LTPT results in Fig. 11, where it can be seen that the three-dimensional results at the lowest roughness height are consistent with the two-dimensional results; at the two larger roughness sizes, the three-dimensional results are a bit more pessimistic. However, taken together, the two sets of data strongly suggest that the Brumby correlation based on having the entire upper surface roughened is a good indicator of the losses in maximum lift capability that will be incurred due to the initial ice buildups on wings and tails that do not have leading-edge devices deployed.

A comparison of the indicated reduction in angle-of-attack margin to stall for the two sets of test results is shown in Fig. 12. The reductions vary from a minimum of 3 deg at the lower roughness heights to around 7 deg at the higher roughness heights, with the three-dimensional results clearly being more

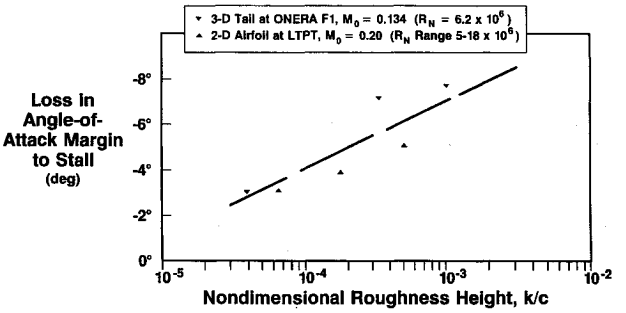

Fig. 12 Comparison of two- and three-dimensional test results for loss in angle-of-attack margin-to-stall due to leading-edge roughness on single-element configurations.

adverse at the larger roughness heights. These reductions need to be addressed when considering the adequacy of stall warning systems when anti-icing protection is not provided.

V. Multielement Airfoil Test Results

To expand upon the study of leading-edge ice (roughness) buildup effects on single-element airfoils in the LTPT, a complementary investigation was undertaken to quantify the degradation of the maximum lift characteristics of a four-element (including two-segment flap) high-lift airfoil configuration resulting from similar small ice (roughness) buildups on the leading-edge slat at approach conditions. As was done with the single-element airfoil, a water impingement analysis was carried out to determine where the distributed roughness should be placed on the slat. Typical results from this water impingement analysis are illustrated in Fig. 13 for an approach condition. On the basis of the impingement analysis, the principal area covered was the initial 4.5% (unextended airfoil) chord on both the upper and lower surfaces of the slat. A photograph of the roughness installation is shown in Fig. 14. To correlate the sensitivity of the maximum lift losses to the extent of the area covered with roughness, an additional configuration with the entire upper surface of the slat covered was also evaluated.

Tests of the four-element high-lift configuration, first without simulated ice, and then with the same three roughness sizes as used in the single-element study, were conducted at a freestream Mach number of 0.20, and at (unextended) chord Reynold numbers of 5 × 10⁶, 9 × 10⁶, and 16 × 10⁶. The resultant degradation in maximum lift capability (for the roughness coverage to 4.5% chord) as a function of the nondimensional roughness height (k/c) is shown in Fig. 15 for the intermediate Reynolds number, compared to the Brumby estimate[1] for configurations with slats extended. The observed (percentage) losses, which, incidentally, are relatively insensitive to Reynolds number variations over the range tested, are much lower than those seen on single-element airfoils. The losses in maximum lift capability range from about 5% at the smallest roughness to just over 10% at the largest, compared to losses of from 20% to over 30% for the single-element cases. However, as will be seen subsequently, the actual reductions in angle-of-attack margin-to-stall are remarkably similar.

The impact of roughness on the slat on the total (four-element) configuration lift characteristics is illustrated in Fig. 16. In addition, the impact on the individual contributions of the slat and main airfoil element is shown. It is the main element that is losing the lift that leads to the reduction in maximum lift capability. Examination of the leading-edge peak suction pressures on both the slat and main element (see Fig. 17) for these cases with roughness on the slat clearly shows that there is an alteration of the flow pattern around the leading edge of the main element concurrent with the flow breakdown on the slat.

As indicated previously, the roughness coverage area with the smallest roughness height (k/c = 0.00007) was also ex-

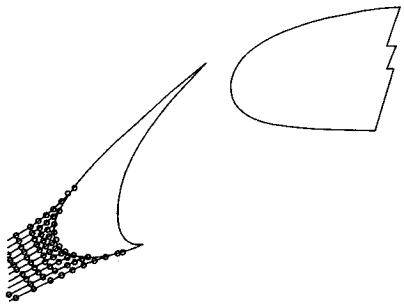

Fig. 13 Analysis of water impingement on slat.

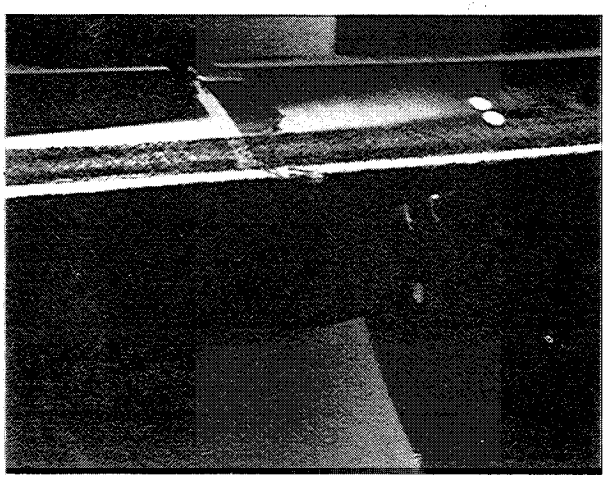

Fig. 14 Roughness applied on slat.

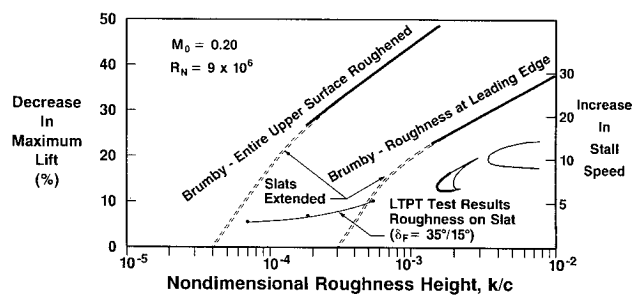

Fig. 15 Effects of roughness on leading-edge slat.

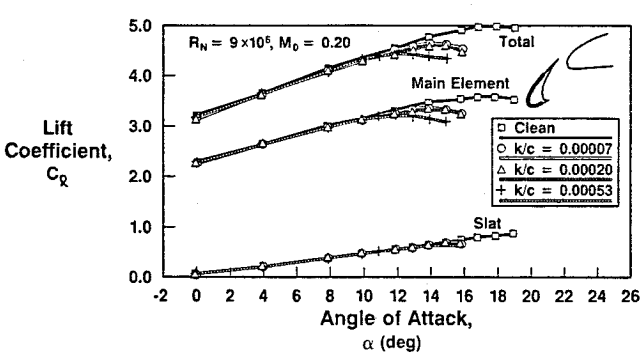

Fig. 16 Effects of slat roughness on four-element airfoil lift characteristics.

tended to cover the entire upper surface of the slat to determine the sensitivity of the measured losses in maximum lift to the extent of the roughened area. The measured lift characteristics for the two coverage patterns are shown in Fig. 18 compared to the clean configuration. It can be seen that there is very little difference in the measured maximum lift characteristics for the two roughness coverage areas. What is clearly

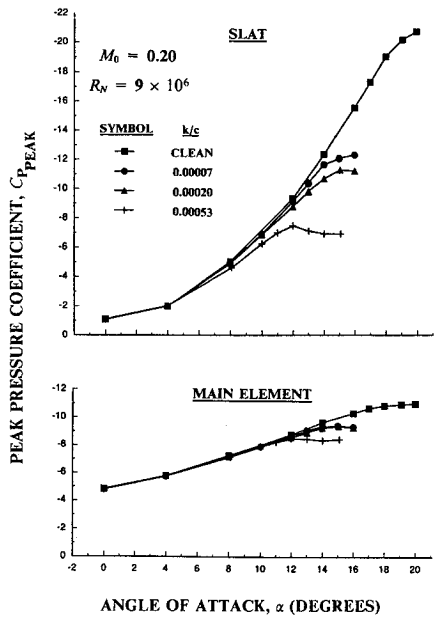

Fig. 17 Effects of slat roughness on peak suction pressures for multielement airfoil.

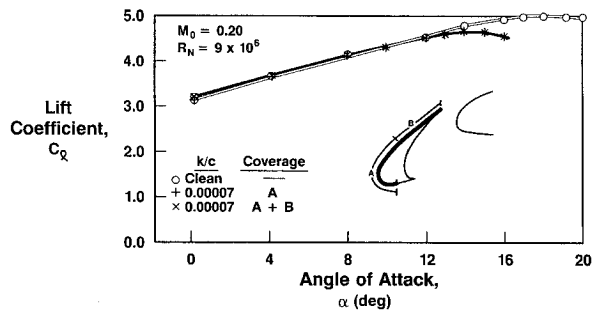

Fig. 18 Effects of slat roughness coverage on four-element airfoil total lift characteristics.

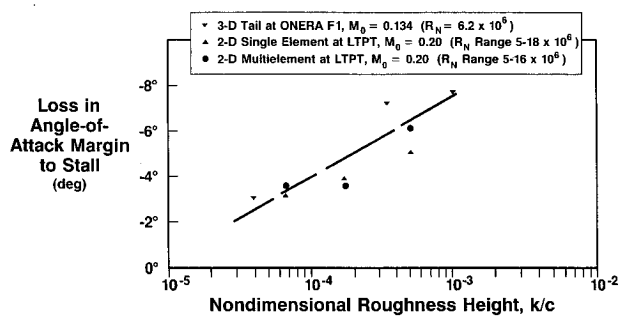

Fig. 19 Correlation of single-element and multielement airfoil test results for loss in angle-of-attack-margin-to-stall due to leading-edge roughness.

dominant in triggering the flow breakdown is locating the roughness elements over the leading-edge region where the suction peak normally develops. Extending the roughness coverage further aft is inconsequential.

A most interesting correlation is observed when comparing the indicated reductions in angle-of-attack margin-to-stall due to the ice (roughness) buildup for this multielement high-lift airfoil case, to the same data for the single-element airfoil cases. It can be seen from Fig. 19 that they are all essentially coincident. Therefore, this correlation provides a relatively quick way to assess the maximum lift penalties incurred for a leading-edge ice (roughness) buildup on any representative wing or tail configuration. It also provides the information needed to check on the adequacy of stall warning systems when anti-icing protection is not provided.

VI. Practical Considerations

It is clear that potential applications of de-icing systems (in lieu of anti-icing systems) for wings and tails of new transport aircraft need to be carefully reassessed in light of the present test results. The identified reductions in maximum lift capability on configurations without leading-edge devices extended are very large, even for extremely small leading-edge ice (roughness) buildups. For example, roughness heights of around 0.005 in. would result in reductions in maximum-lift capability of 20% at the critical spanwise stations on the wing or tail of a representative 200-seat transport. Obviously, the concern is even greater for smaller aircraft. Allowing a leading-edge roughness size of 0.03 in. (perhaps the minimum ice buildup that can be reliably eliminated by a de-icing system) would result in losses in maximum lift capability of up to 40% for the 200-seat aircraft. If the wing or tail surface areas for a particular configuration are sized by maximum lift capability, then corresponding increases in surface areas would be required, with all the attendent performance penalties (drag, weight, etc.).

Lower percentage losses in maximum-lift capability due to leading-edge ice buildups are experienced if the ice buildup occurs on an extended/deflected leading-edge device such as a slat. The maximum-lift penalty for the 0.03-in. ice buildup on a slat would be about 10% at typical landing flap settings. However, the penalty could be near 20% on the wing for lower takeoff flap settings, or for a tail (without deflected flaps). Again, these penalties would all be increased for smaller aircraft. The correlation for reductions in angle-of-attack margin-to-stall as a function of the nondimensional roughness buildup, as presented in Fig. 19, should permit a representative assessment of reductions in maximum lift capability for any relatively conventional configuration. However, if a leading-edge device is to be deployed to reduce the maximum lift penalties due to an initial frost formation, then the impact of the extra drag incurred whenever operating in icing conditions must be taken into account.

VII. Conclusions

A systematic experimental investigation has been carried out to establish the reductions in maximum lift capability that would be incurred by both single-element and multielement aerodynamic surfaces (airfoil, wings, tails, etc.) due to the initial leading-edge ice (roughness) buildup that would occur if de-icing systems are employed. Emphasis in this study was placed on obtaining results at high Reynolds numbers in order to assure the applicability of the finding. Analysis of the results from this investigation has led to the following conclusions:

1) Use of the "Brumby" correlation for the impact of discrete roughness elements at the leading edge of single-element configurations to estimate maximum lift losses is overly optimistic for the representative initial ice (roughness) buildups that occur. However, the correlation for the entire upper surface roughened, which predicts much greater losses, is a good indicator of the losses observed experimentally.

2) Losses in maximum-lift capability of 40% are indicated on single-element configurations for the typical minimum initial ice buildups that can be removed with de-icing systems being studied presently.

3) The authenticity of maximum-lift losses observed in two-dimensional tests at chord Reynolds numbers of 5×10^6 and above has been verified by three-dimensional test results. However, two-dimensional test results obtained at lower Reynolds numbers are misleading. Specifically, at the smallest roughness and the lowest Reynolds number tested, the percent loss in maximum-lift was only 30% of that measured at the higher Reynolds numbers.

4) Lower percentage losses in maximum-lift capability due to leading-edge ice buildups are experienced if the ice buildup occurs on an extended/deflected leading-edge device such as a slat. Losses of from 10 to 20% are indicated, dependent upon whether trailing-edge flaps are deployed or not.

5) A correlation of the reduction in angle-of-attack margin-to-stall due to leading-edge ice buildup has been established which allows the assessment of likely losses in maximum-lift capability for any relatively conventional configuration. Reductions in angle-of-attack margin of 6 deg are indicated for the typical minimum initial ice buildups ($k/c \sim 0.0005$) that could (possibly) be removed by de-icing systems on a representative 200-seat transport.

References

[1]Brumby, R. E., "The Effect of Wing Ice Contamination on Essential Flight Characteristics," Society of Automative Engineers Aircraft Ground De-Icing Conf., Denver, CO, Sept. 20–22, 1988.

[2]Morgan, H. L., Ferris, J. C., and McGhee, R. J., "A Study of High-Lift Airfoils at High Reynolds Numbers in the Langley Low-Turbulence Pressure Tunnel," NASA TM-89125, July 1987.

[3]McGhee, R. J., Beasley, W. D., and Foster, J. M., "Recent Modifications and Calibration of the Langley Low-Turbulence Pressure Tunnel," NASA TP2328, July 1984.

[4]Cebeci, T., and Chang, K. C., "Calculation of Incompressible Rough-Wall Boundary-Layer Flows," *AIAA Journal*, Vol. 16, No. 7, 1978, pp. 730–735.

[5]Hess, J. L., Friedman, D. M., and Clark, R. W., "Calculation of Compressible Flow About Three-Dimensional Inlets with Auxiliary Inlets, Slats, and Vanes by Means of a Panel Method," McDonnell Douglas Rept. J3789, 1985; see also NASA CR-174975, and AIAA Paper 85-1196, June 1985.

[6]Shin, J., Berkowitz, B., Chen, H. H., and Cebeci, T., "Prediction of Ice Shapes and Their Effect on Airfoil Performance," AIAA Paper 91-0264, Jan. 1991.